Membrane-binding properties of gating-modifier and pore-blocking toxins: membrane interaction is not a prerequisite for modification of channel gating

Evelyne Deplazes [1,2 ‡#], Sónia Troeira Henriques [1 ‡], Jennifer J. Smith [1], Glenn F. King [1], David J. Craik [1], Alan E. Mark [2], and Christina I. Schroeder [1#]

[1]Institute for Molecular Bioscience, The University of Queensland, Qld, 4072, Australia.

[2]School of Chemistry and Molecular Biosciences, The University of Queensland, Qld, 4072, Australia.

‡ E.D. and S.T.H. contributed equally to this work.

Corresponding authors:

Dr. Evelyne Deplazes
Institute for Molecular Bioscience
The University of Queensland
St. Lucia, QLD 4072, Australia
Email: e.deplazes@uq.edu.au
Tel: +61 7 336 57562

Dr. Christina I. Schroeder
Institute for Molecular Bioscience
The University of Queensland
St. Lucia, QLD 4072, Australia
Email: c.schroeder@imb.uq.edu.au
Tel: +61 7 334 62021

ABSTRACT

Many venom peptides are potent and selective inhibitors of voltage-gated ion channels, including channels that are validated therapeutic targets for treatment of a wide range of human diseases. However, the development of novel venom-peptide-based therapeutics requires an understanding of their mechanism of action. In the case of voltage-gated ion channels, venom peptides act either as pore blockers that bind to the extracellular side of the channel pore or gating modifiers that bind to one or more of the membrane-embedded voltage sensor domains. In the case of gating modifiers it has been debated whether the peptide must partition in to the membrane to reach its binding site. In this study we used surface plasmon resonance, fluorescence spectroscopy and molecular dynamics to directly compare the lipid binding properties of two gating modifiers (μ-TRTX-Hd1a and ProTx-I) and two pore-blockers (ShK and KIIIA). Only ProTx-I was found to bind to model membranes. Our results provide further evidence that the ability to insert into the lipid bilayer is not a requirement to be a gating modifier. In addition, we characterised the surface of ProTx-I that mediates its interaction with neutral and anionic phospholipid membranes and show that it preferentially interacts with anionic lipids.

Highlights

- The first direct comparison of lipid-binding properties of two pore blockers and two gating modifiers.
- Venom-derived pore blockers do not interact with lipid membranes.
- The venom-derived gating modifier peptide ProTx-I interacts strongly with phospholipid membranes, with a preference for anionic lipid-containing membranes.
- The venom-derived gating modifier Hd1a does not bind to phospholipid membranes.
- Interaction with lipid membranes is not a prerequisite for potent gating-modifier activity.

Keywords:

Venom peptide, toxin, gating modifier, pore blocker, voltage gated ion channel, lipid binding, phospholipid membrane, surface plasmon resonance, molecular dynamics simulations

Abbreviations:

Ca_V	Voltage-gated calcium channel
GMs	Gating modifier, gating modifying peptide
Hd1a	μ-TRTX-Hd1a
K_V	Voltage-gated potassium channel
LUV	Large unilamellar vesicle
Na_V	Voltage-gated sodium channel
PBs	Pore blocker, pore blocking peptide
POPC	1-palmitoyl-2-oleoyl-*sn*-glycero-3-phosphocholine
POPS	1-palmitoyl-2-oleoyl-*sn*-glycero-3-phospho-L-serine
ProTx-I	Protoxin1, β-theraphotoxin-Tp1a
VGICs	Voltage-gated ion channels
VSDs	Voltage-sensing domains
SASA	Solvent accessible surface area
SUV	Small unilamellar vesicle

1. Introduction

Voltage-gated ion channels (VGICs) play crucial roles in diverse physiological processes [1, 2], and are drug targets for a range of diseases, including chronic pain, multiple sclerosis, epilepsy and cardiac arrhythmia [3-5]. Venoms from arachnids, sea anemones, cone snails, and other venomous animals are a rich source of pharmacologically active peptides [6-9] that target VGICs, especially voltage-gated sodium (Na_V), potassium (K_V) and calcium (Ca_V) channels [1, 10-16]. These peptides are often highly potent and selective and have thus attracted much interest as potential lead molecules for pharmaceutical development [17-20]. However, full exploitation of their therapeutic potential requires an understanding of their mechanism of action.

VGICs are transmembrane proteins responsible for the selective transport of ions across cell membranes in response to changes in the membrane potential. They share a common architecture consisting of a central pore domain, responsible for ion conduction, and four voltage-sensing domains (VSDs) that turn the channel on or off in response to changes in the transmembrane potential [1, 21-25]. The gating cycle of VGICs comprises three distinct states: closed (resting), open (activated) and in some cases also an inactivated state. Venom peptides interfere with the gating cycle via two distinct mechanisms. Some peptides inhibit the channel by binding to the pore domain and preventing ion conduction. These peptides are referred to as pore blockers (PBs). Alternatively, some venom peptides can bind to a VSD and alter the kinetics and gating behaviour by changing the relative stability of the closed, open or inactivate states of the channel [16, 21]. Peptides acting via this mechanism are called gating modifiers (GMs). As the pore domain is solvent accessible it is likely that the binding affinity of PBs is primarily governed by peptide-protein interactions and is independent of the lipid environment surrounding the VGIC protein. However, this has not been studied systematically. In contrast, the VSDs are largely buried in the membrane, which potentially prevents gating modifier peptides directly accessing their binding site on the VSD. Thus, gating modification is potentially a three-component system involving the peptide, the VSD and the surrounding lipid membrane. The role of membrane partitioning and specific peptide-lipid interactions in the mechanism of GMs remains an open question. Some studies have shown that

the tarantula toxins VsTx1 [26, 27], SGTx1 [28, 29], hanatoxin [29, 30] and ProTx-II [31, 32], as well as other GMs [31], partition into phospholipid bilayers. This has led to the suggestion that GMs act via a 'membrane-access mechanism' [27]. However, other studies have shown that gating modifier peptides such as huwentoxin-IV [32] do not partition into membranes [31-34] or their binding to the VSD is independent of the ability of the peptide to insert into the lipid bilayer [33]. Furthermore, contradictory results have been reported regarding the requirement of anionic phospholipids for the ability of some gating modifier peptides to insert into lipid membranes. Lee and McKinnon reported that VsTx1 binds to membranes containing some anionic phospholipids and also to membranes comprised solely of zwitterionic phospholipids [27]. In contrast, Jung *et al.* claimed that anionic lipids are essential for membrane partitioning of VsTx1 [26]. Similarly, Milescu *et al.* [29] reported that SGTx1 binds to neutral and anionic phospholipids whereas in a later study Posokhov *et al.* reported that membrane partitioning of SGTx1 only occurs in the presence of anionic lipids [34].

A number of studies have investigated the nature of the interaction between lipids and GMs, including the position of the peptide in the lipid bilayer [26, 28-30, 35-37]. Based on these studies it has been suggested that many gating modifier peptides are localised at the water-lipid interface and that the orientation of the peptide in the membrane and/or specific lipid-peptide interactions might be important for GMs to bind to VSDs. The position of the peptides and their orientation at the water-lipid interface might result from their amphipathic character. Although there is increasing evidence that the originally proposed 'membrane-access mechanism' [27] cannot be generalised to all GMs, to date there has not been a direct comparison of the phospholipid binding activities of PBs and GMs.

In the current study the ability of two PBs and two GMs (Fig. 1) to bind phospholipid bilayers was investigated using surface plasmon resonance (SPR), fluorescence spectroscopy and molecular dynamics (MD) simulations. The two PBs we investigated are: (i) ShK, a 35-residue peptide isolated from the sea anemone *Stichodactyla helianthus* [14, 38-41]. ShK potently blocks Kv1.3 and is currently in Phase IIa clinical trials for the treatment of autoimmune diseases; (ii) KIIIA, a 16-

residue μ-conotoxin isolated from the cone snail *Conus kinoshitai* which inhibits tetrodotoxin-sensitive Na_V channels [42-45]. These two peptides were compared to two GMs: (i) μ-TRTX-Hd1a (Hd1a), a 36-residue peptide isolated from the tarantula *Haplopelma doriae* that selectively inhibits $Na_V1.1$ and $Na_V1.7$ [19] and (ii) ProTx-I, a promiscuous 35-residue peptide isolated from the tarantula *Thrixopelma pruriens* that inhibits Na_V, K_V and Ca_V channels [15, 46, 47]. The interactions of these peptides with phospholipids have not been investigated previously.

Our study shows that PBs exhibit only a weak affinity for lipid membranes. Of the two GMs tested, Hd1a interacted poorly with phospholipid bilayers, whereas ProTx-I showed concentration-dependent binding to both neutral and anionic membranes. Fluorescence spectroscopy measurements and MD simulations of ProTx-I in the presence of phospholipid membranes revealed that the peptide preferentially binds to the water-lipid interface and that residues on or near the hydrophobic face of the peptide probably form the dominant lipid interaction surface of ProTx-I.

2. Materials and methods

2.1. Peptide synthesis

ShK, ProTx-I and KIIIA were chemically synthesised using standard Fmoc solid-phase synthesis protocols using a Symphony peptide synthesiser (Protein Technologies Inc). ShK and ProTx-I were assembled on 2-chlorotrityl resin at 0.25 mmol scale and KIIIA was assembled on rink-amide resin at 0.25 mmol scale to produce an amidated C-terminal. The amino acid protecting groups used were Cys(Trt), Asp(tBu), Glu(tBu), Lys(Boc), Asn(Trt), Arg(Pbf), Ser(tBu), Thr(tBu), Trp(Boc), His(Trt), Gln(Trt) and Tyr(tBu). The peptides were released from the resin and amino acid side chain simultaneously cleaved by incubation with triisopropylsilane (TIPS):H_2O:TFA (2:2:96, v/v/v) for 2.5 h at room temperature. Trifluoroacetic acid (TFA) was evaporated under vacuum, and peptides precipitated with ice-cold diethyl ether. Peptides were dissolved in 50% acetonitrile (0.05% TFA) and lyophilized. The crude linear peptides were purified using reversed phase high-performance liquid chromatography (RP-HPLC) (0–80% B over 80 min, flow rate 8 mL/min, solvent

A; 0.05% TFA, solvent B 90% acetonitrile (ACN)/0.045% TFA on a Shimadzu RP-HPLC) and their molecular mass determined using electrospray mass spectrometry (ESI-MS). Purified peptides were oxidised as described previously for KIIIA [48], ShK [39] and ProTx-I [47]. Recombinant Hd1a was produced as described previously [19]. Peptide purity was >95%, as determined using analytical-HPLC, and the correct disulfide-bond connectivity was established using 1D and 2D NMR spectroscopy. The overall hydrophobicity of the peptides was assessed by comparing the retention times obtained by analytical RP-HPLC using a 2%/min gradient of solvent B (90% ACN/0.1% formic acid) against solvent A (0.1% formic acid).

2.2. Preparation of lipid vesicles

Synthetic phospholipids, 1-palmitoyl-2-oleoyl-*sn*-glycero-3-phosphocholine (POPC) and 1-palmitoyl-2-oleoyl-*sn*-glycero-3-phospho-L-serine (POPS), were purchased from Avanti polar lipids. Lipid films were prepared by solubilising POPC, or a mixture of POPC and POPS (4:1 molar ratio), in chloroform (spectroscopic grade, Sigma); the solvent was evaporated under nitrogen flow and left under vacuum for ~16 h. Small unilamellar vesicles (SUVs, 50 nm diameter) or large unilamellar vesicles (LUVs, 100 nm) composed of POPC or POPC/POPS (4:1) were obtained by hydration of the lipid films with HEPES buffer (10 mM HEPES, 150 mM NaCl, pH 7.4) followed by freeze-thaw fracturing and sizing by extrusion, as described previously [49]. SUVs were used in surface plasmon resonance whereas LUVs were used in fluorescence spectroscopy studies [50].

2.3. Peptide-lipid interactions followed by Surface Plasmon Resonance

Peptide samples were prepared in HEPES buffer and the concentration quantified by absorbance at 280 nm based on extinction coefficients calculated from the contribution of aromatic residues and disulfide bonds as follows: 7365 $M^{-1}.cm^{-1}$ for Hd1a; 18365 $M^{-1}.cm^{-1}$ for ProTx-I; 18365 $M^{-1}.cm^{-1}$ for ShK and 5875 $M^{-1}.cm^{-1}$ for KIIIA.

SPR measurements were conducted at 25 ºC using a Bioacore 3000 instrument (GE Healthcare) with a L1 biosensor chip. All solutions were freshly prepared and filtered (0.22 μm pore); HEPES buffer was used as running buffer. Peptide samples were injected over lipid bilayers deposited

onto the chip surface as described previously [49, 51]. Varying peptide concentrations were tested (1–64 μM) based on the ability of each peptide to bind to a POPC or POPC/POPS (4:1) bilayer. Response units (RU) were converted into mass of peptide or lipid assuming 1 RU=1 pg/mm^2 [52]. The amount of peptide bound to the lipid bilayer was calculated at a reporting point at the end of the association phase (t = 170 s) and normalised to the amount of lipid deposited onto the chip surface and represented as a peptide-to-lipid ratio (P/L; mol/mol) [53]. The ability of a peptide to bind to a membrane of a given lipid composition can be inferred based on the P/L signal obtained at the end of the association curve, and/or on the dissociation rate. Sensorgrams obtained with peptides having low affinity for a certain lipid membrane typically give a SPR binding response of ≤ 0.05 P/L (mol/mol) when injected at concentrations ≥ 30 μM and/or have a very fast dissociation rate reaching P/L close to 0 after 5–10 s of dissociation [51, 54].

2.3 Peptide-lipid interactions followed by fluorescence spectroscopy

Changes in the membrane dipolar potential upon insertion of peptides into the lipid bilayer were examined using the dye 4-[2-[6-(dioctylamino)-2-naphthalenyl]ethenyl]-1-(3-sulfopropyl) (di-8-ANEPPS; Invitrogen) [50]. Fluorescence excitation spectra ($\lambda_{emission}$ = 558 nm) of LUVs composed of 200 μM POPC/POPS (4:1) and 4 μM di-8-ANEPPS were recorded in the absence and presence of 20 μM of each of the four toxins. Differential excitation spectra were calculated as described [50].

ProTx-I is intrinsically fluorescent as it contains three Trp residues. Insertion of these Trp residues into lipid membranes was examined by steady-state fluorescence as described previously [50, 55]. Briefly, 25 μM of ProTx-I was titrated with LUVs composed of POPC/POPS (4:1) up to 4 mM of lipid concentration and fluorescence emission spectra recorded with excitation at 280 nm. Spectra were corrected for the blank, dilution and light dispersion due to addition of LUVs.

Fluorescence emission quenching induced by acrylamide was used to examine whether the Trp residues are solvent exposed. Fluorescence emission intensity (($\lambda_{excitation}$ at 290 nm and $\lambda_{emission}$ at

348 nm) of 25 μM ProTx-I in the absence or presence of 1 mM POPC/POPS (4:1) was followed upon titration with acrylamide up to 100 mM. Data were fitted with the Stern-Volmer equation:

$$\frac{I_0}{I} = 1 + K_{SV}[Q]$$

in which I and I_0 are the fluorescence intensity in the presence and absence of quencher, [Q] is the concentration of quencher and K_{SV} is the Stern-Volmer constant. The quenching efficiency was compared with the calculated K_{SV} as reported [50, 55]. All fluorescence measurements were conducted using a LS50 PerkinElmer fluorescence spectrophotometer using quartz cuvettes with 0.5 cm length path. The peptide concentration range used in fluorescence methodologies is higher than the biological active concentrations due to the detection limits of fluorescence spectroscopy but this should not affect the interpretation of the results under the conditions of the current study.

2.3. Molecular Dynamics simulations

2.3.1.Simulations of ProTx-I in water

Simulations of free peptide in water were performed to ensure the structure was equilibrated before simulating the peptide in the presence of a given lipid bilayer. The ProTx-I NMR structure 2M9L.pdb [56] was used as a starting structure. The peptide was modelled with a NH_3^+ N-terminus and a COO^- C-terminus. Disulfide bonds were modelled according to the NMR structure. Lys and His residues were simulated in their protonated state whereas Asp and Glu were modelled in their de-protonated state. The peptide was placed in a rectangular box and hydrated with water. The net charge was neutralised with Na^+ and Cl^- ions and further ions were added to give a final salt concentration of 100 mM NaCl. The system was energy minimised using a steepest descent algorithm and the solvent was equilibrated by simulating for 2-ns with position restraints on all backbone atoms of the peptide. The unrestrained peptide was simulated for 100 ns in duplicate, in with starting velocities were randomly assigned from Maxwellian distributions. The final conformations of the peptide from these simulations were used as starting structures for the simulations of ProTx-I in the presence of POPC and POPC/POPS (4:1) bilayers.

2.3.2. Simulations of ProTx-I in the presence of a POPC membrane

Four simulation systems were built using the equilibrated peptides and a fully equilibrated lipid bilayer consisting of 128 POPC molecules [57] obtained from the Automatic topology builder (ATB) [58-60]. The peptide was positioned approximately 0.2–0.3 nm from the lipid bilayer in a random orientation. Each system was hydrated with water molecules and the net charge was neutralised with Na^+ and Cl^- ions and further ions were added to give a final salt concentration of 100 mM NaCl. The systems were energy minimised using a steepest descent algorithm and the solvent was equilibrated by simulating for 2-ns with position restraints on all backbone atoms of the peptide and all heavy atoms in the lipid molecules. Each of the four systems were then simulated for 300 ns in duplicate using randomly assigned starting velocities giving a total of eight independent simulations of 300 ns.

2.3.3. Simulations of ProTx-I in the presence of POPC/POPS (4:1)

A POPC/POPS (4:1) bilayer was prepared using the fully equilibrated lipid bilayer consisting of 128 POPC molecules [57] obtained from ATB [58-60]. In each of the two leaflets, 13 randomly selected POPC molecules were replaced with POPS molecules to give a bilayer consisting of 102 POPC and 26 POPS molecules. This POPC/POPS bilayer was solvated with water molecules and the net charge was neutralised with Na^+ and Cl^- ions to give a final salt concentration of 100 mM NaCl. The system was energy minimised using a steepest descent algorithm and equilibrated for 100 ns. This equilibrated bilayer was used to set up four simulation systems of ProTx-I in the presence of POPC/POPS analogous to the simulations of ProTx-I in the presence of POPC. Each of the four systems was simulated for 300 ns giving a total of eight independent simulations of 300 ns.

2.3.4. Simulation parameters

All simulations were performed using GROMACS version 3.3.3 [61], in conjunction with the GROMOS 54A7 force field [62]. Parameters for POPC were taken from the revised GROMOS 53A6 force field for lipids [63, 64]. The topology and parameters for POPS lipids were obtained from ATB [58-60]. Water was described using the simple point charge (SPC) water model [65]. All simulation systems were subjected to periodic boundary conditions using a rectangular box. Non-bonded interactions were evaluated using a twin-range cut-off scheme. Interactions in the short

range were cut-off at 0.8 nm and were calculated every step, whereas interactions in the long-range were cut-off at 1.4 nm and updated every two steps. To minimize the effect of truncating the electrostatic interactions beyond the 1.4 nm long-range cut-off, a reaction field correction was applied using a relative dielectric constant (ε_r) of 78.5 [66]. The reason why a reaction field was chosen to calculate the long range electrostatic was threefold. First, a reaction field is significantly computationally more efficient than lattice sum methods. Second, the force field used was parameterized for use with a 1.4 nm cutoff and reaction field, and third given the cutoff used there is very little difference between a reaction field and a lattice sum method such as PME including for lipid simulations. The SHAKE algorithm [67] was used to constrain covalent bond lengths during the simulation. The simulation temperature was maintained at a temperature of 298 K using a Berendsen thermostat [68] with a coupling constant (τ_P) of 0.1 ps. For simulations of ProTx-I in water, the pressure was maintained at 1 bar by isotropically coupling the system to an external bath using the method of Berendsen [68] with an isothermal compressibility of 4.5×10^{-5} bar^{-1} and τ_P of 1 ps. The Berendsen methods were used as they lead to a continuous trajectory and do not require the introduction of stochastic forces or lead to oscillations. For simulations of ProTx-I in the presence of a POPC and POPC/POPS, an anisotropic pressure coupling using the same parameters as for simulations of ProTx-I in water was used. In all simulations, a 2 fs time step was used and configurations were saved every 100 ps for analysis. All images were produced using VMD [69].

2.3.5. Analysis

Analysis was carried out with GROMACS tools [61] and python scripts using the MDAnalysis package [70]. Prior to analysis all simulation systems were reoriented such that the membrane was aligned in the x-y plane. Electron density profiles were used to determine the depth of the peptide in the lipid bilayer. For this, the density of the lipid head groups, the lipid tails and the peptides across the lipid bilayer (i.e. along the z-axis) was calculated and plotted as a function of the distance from the bilayer centre. The density of the lipid head groups and lipid tails were averaged over the eight independent simulations while the density of the peptide was calculated for each individual simulation.

To estimate the orientation of the peptide when bound to the membrane the angle between the peptide and the membrane surface was calculated. The orientation of the peptide was represented by a plane running through Cα of three residues on opposing sides of the peptide. The surface of the membrane was approximated by the x-y plane of the simulation system. For each independent simulation, the last 200 ns of the trajectory were used to calculate angles as a function of simulation time. From this data, 'box-and-whiskers-plots' were created in which the bottom, middle and top of the box represent the 25^{th}, 50^{th} and 75^{th} percentile, respectively, and the whiskers represent the 10^{th} and 90^{th} percentile.

To determine whether some residues interact more frequently with the lipid bilayer than others, a per-residue analysis of the minimum distance between the peptide and the lipid bilayer was carried out. The last 200 ns of each independent simulation were combined to form a single trajectory for the POPC simulations and another single trajectory for the POPC/POPS simulations. These trajectories were used to calculate a per-residue normalised frequency of finding a given residue within 0.35 nm of a lipid molecule. For example, a normalised frequency of 0.40 for a given residue means that this residue is within 0.35 nm of the lipid bilayer for 40% of the simulation time in the combined trajectory. The average and standard deviation of the normalised frequencies over all residues were calculated and used to identify residues that show a normalised frequency at least one standard deviation above or below the average.

The total and hydrophobic solvent accessible surface area (SASA) of each peptide was calculated using a probe of 0.14 nm. For the hydrophobic SASA only Ala, Leu, Val, Ile, Pro, Phe, Met and Trp resides were used. As these peptides are charged species the dipole is not formally defined. The dipole can be calculated but it is dependent upon the origin of the coordinates i.e. for charged species the dipole is no longer invariant upon translations. However, to make a qualitative comparison between the different peptides we estimated the residual dipole that is invariant of rotation and position in the coordinate system as described by Buckingham [71]. In the tool used in this study (g_dipole found in the GRAOMCS package) this is achieved by subtracting the net

charge at the centre of mass of the molecule. The residual dipole moment of each peptide was estimated using the GROMACS tool g_dipoles, in which the net charge is subtracted at centre of mass of the molecule.

3. Results

The aim of this study was to compare the ability of pore blocking and gating modifier peptides to bind to phospholipid bilayers and determine whether membrane binding is a prerequisite for the activity of GMs. For this study we chose four peptides with pharmacological potential, including two PBs (ShK and KIIIA) and two GMs (Hd1a and ProTx-I) that differ in sequence, source, biophysical properties and molecular target (Fig. 1A).

3.1. Phospholipid binding activity of pore blockers and gating modifiers followed by SPR

SPR was used to compare the affinity of the four peptides for neutral (POPC) and negatively charged (POPC/POPS 4:1) membranes. Cell membranes in eukaryotic cells are in the fluid phase and have an asymmetric phospholipid composition; in particular, the outer leaflet is neutral and mainly composed of phospholipids containing phosphatidylcholine (PC) headgroups, whereas the inner leaflet contains ~20% of negatively-charged phosphatidylserine (PS)-phospholipids in addition to zwitterionic phospholipids (mainly with PC- or phosphatidylethanolamine (PE)-headgroups). Thus, POPC bilayers, fluid at 25 ºC, were used here to mimic the neutral outer leaflet, whereas POPC/POPS bilayers mimic the negatively-charged inner leaflet. As mentioned above, some gating-modifier toxins have been proposed to only bind to anionic bilayers, which suggests that the VSD binding site for these toxins might be close to the cytoplasmic leaflet.

Sensorgrams and dose-response curves revealed that both pore-blocking peptides, ShK and KIIIA, have low affinity for POPC and POPC/POPS bilayers (Fig. 2), indicative of a weak ability to bind and/or insert into lipid membranes. Comparison of the sensorgrams obtained with the two gating modifier peptides revealed that ProTx-I binds strongly to both neutral and anionic lipid membranes, whereas Hd1a binds only weakly to POPC and POPC/POPS bilayers (Fig. 2A). ProTx-I had higher

affinity, for anionic membranes (Fig. 2B), possibly due to increased electrostatic attractions between the positively-charged peptide and negatively-charged bilayer. Although all four peptides included in this study have a net positive charge (Fig. 1A), ProTx-1 has the smallest net charge (+2) and yet is the only peptide that binds significantly to anionic membranes. Interestingly, ProTx-I is the most hydrophobic peptide, as assessed by RP-HPLC retention time (Fig. 1A).

3.2. Insertion of toxins into phospholipid bilayers followed by fluorescence spectroscopy

Insertion of peptides into lipid membranes can induce changes in the membrane dipolar potential, which can be monitored by a shift in the fluorescence excitation spectrum of the dye di-8-ANEPPS [50]. Hence, to examine whether any of the venom peptides insert into the membrane, fluorescence excitation spectra of POPC/POPS (4:1) vesicles labelled with di-8-ANEPPS were recorded in the absence and presence of 20 μM of each peptide (Fig. 3A). Even at concentrations much higher than required to inhibit channel activity, ShK, KIIA and Hd1a did not induce changes in the fluorescence excitation spectrum of di-8-ANEPPS, as expected based on their inability to bind to POPC/POPS (4:1) membranes measured by SPR. Interestingly, ProTx-I also did not change the fluorescence excitation properties of di-8-ANEPPS; this result suggests that ProTx-I does not insert deeply in the membrane, and instead might be adsorbed at the membrane interface.

The fluorescence emission of Trp is sensitive to polar/apolar environment [50]; thus, to gain further information on the depth that the Trp residues penetrate into the membrane when ProTx-I is bound to lipid bilayers we followed the Trp fluorescence in the absence and presence of lipid vesicles. The fluorescence emission spectrum of ProTx-I (Fig. 3B) did not change upon titration with POPC/POPS (4:1) LUVs suggesting that the Trp residues do not insert deeply into the membrane [50].

Acrylamide is an aqueous soluble fluorescence quencher unable to insert into lipid membranes and thus it selectively quenches Trp residues exposed to an aqueous environment. Identical ProTx-I fluorescence emission quenching efficiency by acrylamide in the absence and presence of

POPC/POPS (4:1) vesicles (Fig. 3C) also support the hypothesis that Trp residues within ProTx-I do not insert deeply into the lipid bilayer.

3.3. Simulations of ProTx-I in the presence of POPC

We used MD simulations to model the interaction of ProTx-I with POPC bilayers in order to gain information about the depth and orientation of ProTx-I in the membrane, and to identify regions of the peptide that mediate its interaction with lipids. Eight independent 300-ns simulations of ProTx-I in the presence of POPC bilayers were performed. In all simulations, the peptide freely diffuses in the aqueous phase for ~50 ns before binding to the membrane. ProTx-I is stabilised by three disulfide bonds arranged in an inhibitory cystine knot (ICK) motif, which provides the peptide with high structural stability [72]. To check that the peptide is as rigid in the presence of a lipid bilayer as it is in solution we compared the structure of the peptide in the two environments. The heavy-atom Root-Mean Square Deviation (RMSD) as a function of time from the simulation of the peptide in water was compared to the RMSD from the simulations of the peptide in the presence of POPC. In water the peptide shows an average RMSD of 0.09 ± 0.04 nm (average ± 1 standard deviation) and in the presence of POPC the average RMSD is 0.09 ± 0.02 nm. This indicates that the binding of the peptide to the lipid bilayer does not induce any changes in the overall fold of the peptide.

The depths to which the peptide penetrated the membrane were estimated by calculating density profiles of the lipid head groups, lipid carbon tails and peptide along the normal of the membrane (Fig. 4A). The data suggest that ProTx-I spends the majority of the time at the water-lipid interface, partially buried in the lipid head group region and partially exposed to the aqueous environment (Fig. 4C and 4D). Occasionally, part of the peptide inserts into the hydrophobic core of the bilayer. This position of the peptide is consistent with the observation from the fluorescence experiments.

The orientation of the peptide when bound to the membrane was estimated by calculating the angle between the peptide and the surface of the lipid bilayer from the eight independent simulations (Fig. 4B), after the peptide was equilibrated for 100 ns in each simulation system. An orientation angle >45º is indicative of the peptide lying relatively flat on the membrane surface

(Fig. 4C) whereas an orientation angle <45° indicates a more upright position (Fig. 4D). Box plots indicate that the peptide did not adopt a preferred orientation over the timescale of the simulations. However, in most orientations adopted by the peptide the hydrophobic residues Trp5, Leu6, Gly7, Trp27 and Trp30, which are clustered on one face of the peptide (white in Fig. 4C and 4D), mostly pointed towards the lipid headgroups, whereas the polar residues (shown in green) were more likely to be water exposed. These hydrophobic residues form part of the hydrophobic face of ProTx-I (residues Trp5, Leu6, Gly7, Gly8, Gly26, Trp27, Val 29, Trp30 and Phe34; see Fig. 1B). When bound to the membrane the number of POPC molecules within 0.5 nm of the peptide fluctuates between 3 and 20. Averaged over the 8*300 ns of simulations there are 6–8 lipid molecules close to the peptide and further analysis of the lipid residency around the peptide showed that the peptide forms stable interactions with a number of selected lipid molecules rather than short-lived interactions with alternating lipids. This suggests that once the peptide is bound it is 'dragged' along the membrane surface by the diffusing lipids.

To quantitatively assess whether some residues are more likely to interact with the lipid bilayer, we calculated the normalised frequency of finding a residue within 0.35 nm of a lipid molecule (Fig. 5A). This analysis revealed that residues Glu1, Cys2, Tyr4, Trp5, Leu6, Cys16, Lys17 and Tpr30 are more likely to be close to the lipid bilayer (marked with asterisks in Fig. 5A). Notably, Trp5, Leu6 and Trp30 account for 77% of the solvent accessible surface area of the hydrophobic face of the peptide. Residues Leu19, Val20, Cys21, Ser22, Arg23, Cys28 and Thr33 are, on average, less likely to interact with the lipid bilayer. These residues are located on the more polar face of the peptide situated opposite the hydrophobic surface (see Fig. 1B). Collectively, the simulation results suggest that ProTx-I is localised at the water-lipid interface of the POPC membrane with the majority of the hydrophobic face buried in the lipid headgroups, whereas the polar face of the molecule is exposed to the aqueous environment.

3.3. Simulations of ProTx-I in the presence of POPC/POPS (4:1)

The SPR data showed that ProTx-I exhibits a stronger affinity for, and a slower dissociation rate from, membranes that contain anionic phospholipids. To investigate the effect of anionic lipids on

the lipid-ProTx-I interaction, we carried out MD simulations of ProTx-I in the presence of a POPC/POPS (4:1) lipid bilayer. As with the simulations in the presence of POPC, the peptide remained as rigid upon binding to the POPC-POPS bilayer as in solution. The average RMSD of the peptide in the presence of POPC-POPS bilayer is 0.09 ± 0.03 nm (average ± 1 standard deviation) while in water it is 0.09 ± 0.04 nm. In all eight simulations, the peptide bound to the lipid bilayer within the first 10 ns, significantly faster than in simulations with pure POPC. The membrane depth, relative orientation and interaction surface of the peptide were calculated as described for the simulations with pure POPC. The density profiles extracted from the POPC/POPS simulations (Fig. 6A) show that the depth of the peptide is not affected by the presence of the negatively charged lipids. Comparison of the range of angles adopted by the peptides across the eight independent simulations in the presence of zwitterionic (Fig. 4B) and charged lipids (Fig. 6B) showed that the peptide samples a similar range of relative orientations in the two lipid environments. However, the variation within a given simulation is reduced in the presence of anionic lipids suggesting that peptide binds tighter to the surface. Indeed, analysis of the time-dependent orientation of the peptide showed that in the presence of charged lipids the peptides remains longer in a given orientation. Per-residue analysis of the lipid interactions (Fig. 6C) showed that residues Glu1, Cys2, Tyr4, Lys17, His18 and Trp30 are more likely to be close to the membrane while residues Cys9, Cys21, Ser22, Arg23, Cys28 and Val29 are less likely to be in contact with the lipids. It is interesting to note that even in the presence of anionic POPS, the positively charged residues Arg23 and Arg24 show little interaction with the membrane surface. The arginine residues are located on the more polar face of the peptide, suggesting that while the presence of anionic lipids enhances the rate of association of the toxin with the membrane, burial of hydrophobic residues is the main driving force that determines the relative orientation of ProTx-I on the membrane. This is consistent with the fact that there was no increase in the number of POPS molecules around the peptide. That is, the ratio of POPC and POPS lipids within 0.5 nm of the peptide is, on average, the same as in the bulk of the lipid. Comparison of the normalised lipid-residency frequencies for ProTx-I in the presence of POPC only (Fig. 5A) and POPC/POPS (Fig. 6C) shows that Lys17, His18 and Trp30 interact more frequently with membranes containing anionic lipids. Overall there is a large overlap between ProTx-I residues that form the interaction

surface with POPC and POPC/POPS. Residues Glu1, Cys2, Tyr4, Trp5, Lys17 and Trp30 frequently interact with both POPC and POPC/POPS membranes (Fig. 5A and 6C) and likely form the dominant lipid interaction surface of ProTx-I (Fig. 5D). Collectively, the data suggest that in presence of POPC or POPC/POPS the peptide sits at the water-lipid interface with its hydrophobic face buried in the bilayer and the more polar face exposed to solvent. The overall relative orientation of the peptide is very similar but the presence of anionic lipids appears to have a slight anchoring effect. The faster partitioning and 'anchoring' effect in the presence of anionic lipids is consistent with the increased binding affinity and slower off-rates observed in the SPR experiments.

4. Discussion

Disulfide-rich peptides isolated from animal venoms typically have well-defined three-dimensional structures and remarkable stability [6-9]. Many of these peptides inhibit human VGICs with exquisite selectivity and high potency [11, 12, 15, 19]. Consequently, many venom peptides have been investigated as potential insecticides or therapeutics and as pharmacological tools to study the (patho)physiology of VGICs [11-14, 16-18, 73] . Venom peptides can act as PBs, inhibiting the flow of ions through VGICs by blocking the extracellular face of the channel pore, or they can act as GMs by stabilising particular states in the gating cycle via interactions with the membrane-embedded VSDs. It has been proposed that GMs act via a 'membrane-access' mechanism in which lipid binding is a prerequisite for interaction with their cognate VSDs [27]. However, the generality of this mechanism has been questioned [31, 33, 34]. Here we examined the potential of two PBs, KIIIA and ShK, and two GMs, Hd1a and ProTx-I, to bind to neutral and anionic phospholipid membranes. SPR analysis indicated that neither Hd1a nor either of the two PBs interacted with neutral or anionic lipid bilayers. Only ProTx-I interacted significantly with model membranes. Hd1a potently inhibits the human $Na_V1.7$ channel (IC_{50} ~ 110 nM) via interaction with the domain II VSD [19]. This is in agreement with previous studies which reported that other GMs including anthopleurin B (ApB) and *Leiurus* toxin V (LqqV) [31], huwentoxin-IV [32] and HpTx2 [34] showed only weak or no binding to phospholipid membranes. The combined data provide further

evidence that membrane partitioning is not an intrinsic property of all GMs and that the 'membrane-access' mechanism cannot be generalised.

The availability of data on the lipid-binding activity of a number of venom peptides allows a comparison of their structural and chemical properties to help elucidate why only selected GMs bind to membranes. It has been suggested that the membrane partitioning of certain GMs is a consequence of their amphipathic surface profile in which one face of the peptide contains a cluster of hydrophobic residues surrounded by polar, mainly basic, residues [26, 28-31, 35, 37]. Fig. 7 compares the surface composition of two PBs and six gating modifier peptides while Table 1 lists the overall charge, the total and hydrophobic solvent accessible surface areas and the residual dipole moments of the six gating modifier peptides and the two pore blocking peptides investigated in this study.

The GMs Hd1a and huwentoxin-IV [32] do not bind to phospholipid membranes whereas the four GMs VsTx1 [26, 27], SGTx1 [28, 29], hanatoxin [30] and ProTx-I show membrane partitioning. Despite the distinctly different membrane-binding properties of these GMs, they are all amphipathic with a hydrophobic cluster and surface-exposed anionic and cationic residues. Furthermore, the peptides have similar overall charge and their hydrophobic solvent accessible surface area (SASA) as a percentage of total SASA are very similar. While Hd1a and huwentoxin-IV have a higher residual dipole moment than the GMs that do not bind to membranes, a comparison of a much larger set of peptides is needed to determine whether the residual dipole moment can be used to reliably predict the phospholipid binding activity of a peptide. Taken together, these results suggest that the ability of gating modifier peptides to bind membranes cannot be predicted based solely on the presence of a hydrophobic cluster and the amphipathic nature of the peptide, the overall charge of the peptide or its residual dipole moment.

Although the presence of a hydrophobic and polar face might in itself not be sufficient to predict that a given peptide will bind weakly or strongly to lipid membranes, there is evidence that, for those GMs that do partition into membranes, their amphipathic nature determines their position

on/in the membrane. Our fluorescence measurements suggest that ProTx-I binds at the water-lipid interface and MD simulations suggest that the peptide has its hydrophobic face buried in the lipid headgroups with its polar face exposed to the solvent. This is consistent with a number of previous studies that investigated membrane partitioning of the GMs VsTx1, SGTx1 and hanatoxin using a range of experimental techniques and/or MD simulations [26, 28, 30, 35, 37]. In the case of ProTx-I, residues Glu1, Cys2, Tyr4, Trp5, Lys17 and Trp30 appear to form the dominant lipid interaction surface of ProTx-I in the presence of both neutral and anionic phospholipid membranes. These residues form a distinctly different surface than the pharmacophore that mediates the interaction of ProTx-I with Nav1.2 and the transient receptor potential ankyrin 1 (TRPA1) channel [56].

5. Conclusions

In this study, we compared the lipid-binding propensity of venom-derived PBs and GMs. None of the PBs interacted significantly with lipid membranes, consistent with their solvent-exposed extracellular binding site. Although some GMs are able to bind and insert into membranes, we provide evidence that this is not a prerequisite for gating modification via interaction with voltage sensor domains. We have shown that the gating-modifier ProTx-I binds to both neutral and anionic phospholipids. The peptide does not insert deeply into the lipid bilayer but binds to the water-lipid interface, with its hydrophobic face buried in the lipid headgroups and its polar face exposed to the solvent.

Acknowledgments and author contributions

This work was supported by the Australian National Health and Medical Research (NHMRC) in the form of a project grant to C.I.S. and S.T.H. (APP1080405), Early Career Fellowship to E.D (APP1071293), Principal Research Fellowship to D.J.C. (APP1026501), and a project grant (APP1034958) and Principal Research Fellowship (APP1044414) to G.F.K. This research was undertaken with the assistance of resources provided at the NCI National Facility systems at the Australian National University through the National Computational Merit Allocation Scheme

supported by the Australian Government. The authors thank Olivier Cheneval, Phillip Walsh, Timothy Hill for peptide synthesis and peptide expression. E.D., S.T.H. and C.I.S. designed the study. E.D. carried out molecular modelling and S.T.H. performed the surface plasmon resonance and the fluorescence spectroscopy studies. J.S. prepared the Hd1a peptide. E.D., S.T.H. and C.I.S. co-wrote the manuscript and D.J.C, G.F.K and A.M assisted with data interpretation and manuscript editing.

References

[1] W.A. Catterall, Voltage-gated sodium channels at 60: Structure, function and pathophysiology, J. Physiol., 590 (2012) 2577-2589.
[2] F.H. Yu, V. Yarov-Yarovoy, G.A. Gutman, W.A. Catterall, Overview of molecular relationships in the voltage-gated ion channel superfamily, Pharmacol. Rev., 57 (2005) 387-395.
[3] J.G. McGivern, Advantages of voltage-gated ion channels as drug targets, Expert Opin. Ther. Targets, 11 (2007) 265-271.
[4] D.J. Triggle, Voltage-gated ion channels as drug targets, Wiley-VCH, Weinheim, 2006.
[5] H. Wulff, N.A. Castle, L.A. Pardo, Voltage-gated potassium channels as therapeutic targets, Nat. Rev. Drug Discov., 8 (2009) 982-1001.
[6] B. Frazão, V. Vasconcelos, A. Antunes, Sea anemone (cnidaria, anthozoa, actiniaria) toxins: An overview, Mar. Drugs, 10 (2012) 1812-1851.
[7] V. Herzig, D.L. Wood, F. Newell, P.A. Chaumeil, Q. Kaas, G.J. Binford, G.M. Nicholson, D. Gorse, G.F. King, Arachnoserver 2.0, an updated online resource for spider toxin sequences and structures, Nucleic Acids Res., 39 (2011) D653-657.
[8] R. Lewis, S. Dutertre, I. Vetter, M. Christie, Conus venom peptide pharmacology, Pharmacol Rev., 64 (2012) 259-298.
[9] L.D. Rash, W.C. Hodgson, Pharmacology and biochemistry of spider venoms, Toxicon, 40 (2002) 225-254.
[10] P.T. Huang, Y.S. Shiau, K.L. Lou, The interaction of spider gating modifier peptides with voltage-gated potassium channels, Toxicon, 49 (2007) 285-292.
[11] J.K. Klint, S. Senff, D.B. Rupasinghe, S.Y. Er, V. Herzig, G.M. Nicholson, G.F. King, Spider-venom peptides that target voltage-gated sodium channels: Pharmacological tools and potential therapeutic leads, Toxicon, 60 (2012) 478-491.
[12] O. Knapp, J.R. McArthur, D.J. Adams, Conotoxins targeting neuronal voltage-gated sodium channel subtypes: Potential analgesics?, Toxins (Basel), 4 (2012) 1236-1260.
[13] Y. Moran, D. Gordon, M. Gurevitz, Sea anemone toxins affecting voltage-gated sodium channels - molecular and evolutionary features, Toxicon, 54 (2009) 1089-1101.
[14] R.S. Norton, M.W. Pennington, H. Wulff, Potassium channel blockade by the sea anemone toxin ShK for the treatment of multiple sclerosis and other autoimmune diseases, Curr. Med. Chem., 11 (2004) 3041-3052.
[15] B.T. Priest, K.M. Blumenthal, J.J. Smith, V.A. Warren, M.M. Smith, ProTx-I and ProTx-II: Gating modifiers of voltage-gated sodium channels, Toxicon, 49 (2007) 194-201.
[16] K.J. Swartz, Tarantula toxins interacting with voltage sensors in potassium channels, Toxicon, 49 (2007) 213-230.
[17] G F. King, Venoms as a platform for human drugs: Translating toxins into therapeutics, Expert Opin. Biol. Ther., 11 (2011) 1469-1484.
[18] G F. King, Venoms to drugs The Royal Society of Chemistry, Cambridge (UK), 2015.
[19] J.K. Klint, J.J. Smith, I. Vetter, D.B. Rupasinghe, S.Y. Er, S. Senff, V. Herzig, M. Mobli, R.J. Lewis, F. Bosmans, G.F. King, Seven novel modulators of the analgesic target NaV1.7 uncovered using a high-throughput venom-based discovery approach, Br. J. Pharmacol., 172 (2015) 2445-2458.
[20] N.J. Saez, S. Senff, J.E. Jensen, S.Y. Er, V. Herzig, L.D. Rash, G.F. King, Spider-venom peptides as therapeutics, Toxins (Basel), 2 (2010) 2851-2871.
[21] F. Bosmans, K.J. Swartz, Targeting sodium channel voltage sensors with spider toxins, Trends Pharmacol. Sci., 31 (2010) 175-182.
[22] D.A. Doyle, J. Morais Cabral, R.A. Pfuetzner, A. Kuo, J.M. Gulbis, S.L. Cohen, B.T. Chait, R. MacKinnon, The structure of the potassium channel: Molecular basis of K^+ conduction and selectivity, Science, 280 (1998) 69-77.

[23] Y. Jiang, A. Lee, J. Chen, V. Ruta, M. Cadene, B.T. Chait, R. MacKinnon, X-ray structure of a voltage-dependent K^+ channel, Nature, 423 (2003) 33-41.
[24] Y. Li-Smerin, K.J. Swartz, Gating modifier toxins reveal a conserved structural motif in voltage-gated Ca^{2+} and K^+ channels, Proc. Natl. Acad. Sci. U. S. A., 95 (1998) 8585-8589.
[25] S.B. Long, E.B. Campbell, R. Mackinnon, Crystal structure of a mammalian voltage-dependent shaker family K^+ channel, Science, 309 (2005) 897-903.
[26] H.J. Jung, J.Y. Lee, S.H. Kim, Y.-J. Eu, S.Y. Shin, M. Milescu, K.J. Swartz, J.I. Kim, Solution structure and lipid membrane partitioning of VSTx1, an inhibitor of the kvap potassium channel, Biochemistry, 44 (2005) 6015-6023.
[27] S. Lee, R. MacKinnon, A membrane-access mechanism of ion channel inhibition by voltage sensor toxins, Nature, 430 (2004) 232-235.
[28] H.H. Jung, H.J. Jung, M. Milescu, C.W. Lee, S. Lee, J.Y. Lee, Y.J. Eu, H.H. Kim, K.J. Swartz, J.I. Kim, Structure and orientation of a voltage-sensor toxin in lipid membranes, Biophys. J., 99 (2010) 638-646.
[29] M. Milescu, J. Vobecky, S.H. Roh, S.H. Kim, H.J. Jung, J.I. Kim, K.J. Swartz, Tarantula toxins interact with voltage sensors within lipid membranes, J. Gen. Physiol., 130 (2007) 497-511.
[30] L.R. Phillips, M. Milescu, Y. Li-Smerin, J.A. Mindell, J.I. Kim, K.J. Swartz, Voltage-sensor activation with a tarantula toxin as cargo, Nature, 436 (2005) 857-860.
[31] J.J. Smith, S. Alphy, A.L. Seibert, K.M. Blumenthal, Differential phospholipid binding by site 3 and site 4 toxins: Implications for structural variability between voltage-sensitive sodium channel domains, J. Biol. Chem., 280 (2005) 11127-11133.
[32] Y. Xiao, X. Luo, F. Kuang, M. Deng, M. Wang, X. Zeng, S. Liang, Synthesis and characterization of huwentoxin-IV, a neurotoxin inhibiting central neuronal sodium channels, Toxicon, 51 (2008) 230-239.
[33] L. Cohen, N. Gilles, I. Karbat, N. Ilan, D. Gordon, M. Gurevitz, Direct evidence that receptor site-4 of sodium channel gating modifiers is not dipped in the phospholipid bilayer of neuronal membranes, J. Biol. Chem., 281 (2006) 20673-20679.
[34] Y.O. Posokhov, P.A. Gottlieb, M.J. Morales, F. Sachs, A.S. Ladokhin, Is lipid bilayer binding a common property of inhibitor cysteine knot ion-channel blockers?, Biophys. J., 93 (2007) L20-L22.
[35] D. Bemporad, Z.A. Sands, C.L. Wee, A. Grottesi, M.S. Sansom, VSTx1, a modifier of Kv channel gating, localizes to the interfacial region of lipid bilayers, Biochemistry, 45 (2006) 11844-11855.
[36] M. Nishizawa, K. Nishizawa, Interaction between K^+ channel gate modifier hanatoxin and lipid bilayer membranes analyzed by molecular dynamics simulation, Eur. Biophys. J., 35 (2006) 373-381.
[37] C.L. Wee, D. Bemporad, Z.A. Sands, D. Gavaghan, M.S.P. Sansom, SGTx1, a Kv channel gating-modifier toxin, binds to the interfacial region of lipid bilayers, Biophys. J., 92 (2007) L07-L09.
[38] O. Castaneda, V. Sotolongo, A.M. Amor, R. Stocklin, A.J. Anderson, A.L. Harvey, A. Engstrom, C. Wernstedt, E. Karlsson, Characterization of a potassium channel toxin from the caribbean sea anemone stichodactyla helianthus, Toxicon, 33 (1995) 603-613.
[39] M.W. Pennington, M.E. Byrnes, I. Zaydenberg, I. Khaytin, J. de Chastonay, D.S. Krafte, R. Hill, V.M. Mahnir, W.A. Volberg, W. Gorczyca, et al., Chemical synthesis and characterization of ShK toxin: A potent potassium channel inhibitor from a sea anemone, Int. J. Pept. Protein Res., 46 (1995) 354-358.
[40] M.W. Pennington, V.M. Mahnir, I. Khaytin, I. Zaydenberg, M.E. Byrnes, W.R. Kem, An essential binding surface for ShK toxin interaction with rat brain potassium channels, Biochemistry, 35 (1996) 16407-16411.
[41] J.E. Tudor, P.K. Pallaghy, M.W. Pennington, R.S. Norton, Solution structure of ShK toxin, a novel potassium channel inhibitor from a sea anemone, Nat. Struct. Biol., 3 (1996) 317-320.

[42] K.K. Khoo, Z.-P. Feng, B.J. Smith, M.-M. Zhang, D. Yoshikami, B.M. Olivera, G. Bulaj, R.S. Norton, Structure of the analgesic μ-conotoxin KIIIA and effects on the structure and function of disulfide deletion, Biochemistry, 48 (2009) 1210-1219.
[43] J.R. McArthur, G. Singh, D. McMaster, R. Winkfein, D.P. Tieleman, R.J. French, Interactions of key charged residues contributing to selective block of neuronal sodium channels by μ-conotoxin KIIIA, Mol. Pharmacol., 80 (2011) 573-584.
[44] M.-M. Zhang, B.R. Green, P. Catlin, B. Fiedler, L. Azam, A. Chadwick, H. Terlau, J.R. McArthur, R.J. French, J. Gulyas, J.E. Rivier, B.J. Smith, R.S. Norton, B.M. Olivera, D. Yoshikami, G. Bulaj, Structure/function characterization of μ-conotoxin KIIIA, an analgesic, nearly irreversible blocker of mammalian neuronal sodium channels, J. Biol. Chem., 282 (2007) 30699-30706.
[45] A. Van Der Haegen, S. Peigneur, J. Tytgat, Importance of position 8 in mu-conotoxin KIIIA for voltage-gated sodium channel selectivity, FEBS J., 278 (2011) 3408-3418.
[46] C. Bladen, J. Hamid, I. Souza, G. Zamponi, Block of t-type calcium channels by protoxins i and ii, Molecular Brain, 7 (2014) 36.
[47] R.E. Middleton, V.A. Warren, R.L. Kraus, J.C. Hwang, C.J. Liu, G. Dai, R.M. Brochu, M.G. Kohler, Y.D. Gao, V.M. Garsky, M.J. Bogusky, J.T. Mehl, C.J. Cohen, M.M. Smith, Two tarantula peptides inhibit activation of multiple sodium channels, Biochemistry, 41 (2002) 14734-14747.
[48] G. Bulaj, P.J. West, J.E. Garrett, M. Watkins, M.M. Zhang, R.S. Norton, B.J. Smith, D. Yoshikami, B.M. Olivera, Novel conotoxins from conus striatus and conus kinoshitai selectively block TTX-resistant sodium channels, Biochemistry, 44 (2005) 7259-7265.
[49] S.T. Henriques, L.K. Pattenden, M.-I. Aguilar, M.A.R.B. Castanho, PrP(106-126) does not interact with membranes under physiological conditions, Biophys. J., 95 (2008) 1877-1889.
[50] S.T. Henriques, L.K. Pattenden, M.-I. Aguilar, M.A.R.B. Castanho, The toxicity of prion protein fragment PrP(106−126) is not mediated by membrane permeabilization as shown by a M112W substitution, Biochemistry, 48 (2009) 4198-4208.
[51] S.T. Henriques, Y.-H. Huang, K.J. Rosengren, H.G. Franquelim, F.A. Carvalho, A. Johnson, S. Sonza, G. Tachedjian, M.A.R.B. Castanho, N.L. Daly, D.J. Craik, Decoding the membrane activity of the cyclotide kalata B1: The importance of phosphatidylethanolamine phospholipids and lipid organization on hemolytic and anti-HIV activities J. Biol. Chem., 286 (2011) 24231-24241.
[52] M.A. Cooper, A. Hansson, S. Lofas, D.H. Williams, A vesicle capture sensor chip for kinetic analysis of interactions with membrane-bound receptors, Anal. Biochem., 277 (2000) 196-205.
[53] L. Sando, S.T. Henriques, F. Foley, S.M. Simonsen, N.L. Daly, K.N. Hall, K.R. Gustafson, M.I. Aguilar, D.J. Craik, A synthetic mirror image of kalata B1 reveals that cyclotide activity is independent of a protein receptor, ChemBioChem, 12 (2011) 2456-2462.
[54] S.T. Henriques, Y.H. Huang, M.A. Castanho, L.A. Bagatolli, S. Sonza, G. Tachedjian, N.L. Daly, D.J. Craik, Phosphatidylethanolamine binding is a conserved feature of cyclotide-membrane interactions, J. Biol. Chem., 287 (2012) 33629-33643.
[55] I.M. Torcato, Y.H. Huang, H.G. Franquelim, D. Gaspar, D.J. Craik, M.A. Castanho, S.T. Henriques, Design and characterization of novel antimicrobial peptides, R-BP100 and RW-BP100, with activity against Gram-negative and Gram-positive bacteria, Biochim. Biophys. Acta, 1828 (2013) 944-955.
[56] J. Gui, B. Liu, G. Cao, A M. Lipchik, M. Perez, Z. Dekan, M. Mobli, N L. Daly, P F. Alewood, L L. Parker, G F. King, Y. Zhou, S. Jordt, M N. Nitabach, A tarantula-venom peptide antagonizes the TRPA1 nociceptor ion channel by binding to the s1–s4 gating domain, Curr. Biol., 24 (2014) 473-483.

[57] D. Poger, A.E. Mark, On the validation of molecular dynamics simulations of saturated and cis-monounsaturated phosphatidylcholine lipid bilayers: A comparison with experiment, J. Chem. Theory Comput., 6 (2010) 325-336.
[58] S. Canzar, M. El-Kebir, R. Pool, K. Elbassioni, A.E. Mark, D.P. Geerke, L. Stougie, G.W. Klau, Charge group partitioning in biomolecular simulation, J. Comput. Biol., 20 (2013) 188-198.
[59] K.B. Koziara, M. Stroet, A.K. Malde, A.E. Mark, Testing and validation of the automated topology builder (ATB) version 2.0: Prediction of hydration free enthalpies, J. Comput.-Aided Mol. Des., 28 (2014) 221-233.
[60] A.K. Malde, L. Zuo, M. Breeze, M. Stroet, D. Poger, P.C. Nair, C. Oostenbrink, A.E. Mark, An automated force field topology builder (ATB) and repository: Version 1.0, J. Chem. Theory Comput., 7 (2011) 4026-4037.
[61] D. van der Spoel, E. Lindahl, B. Hess, G. Groenhof, A.E. Mark, H.J.C. Berendsen, GROMACS: Fast, flexible and free J. Comput. Chem., 26 (2005) 1701-1718.
[62] N. Schmid, A.P. Eichenberger, A. Choutko, S. Riniker, M. Winger, A.E. Mark, W.F. van Gunsteren, Definition and testing of the GROMOS force-field versions 54a7 and 54b7, Eur. Biophys. J., 40 (2011) 843-856.
[63] D. Poger, A.E. Mark, Lipid bilayers: The effect of force field on ordering and dynamics, J. Chem. Theory Comput., 8 (2012) 4807-4817.
[64] D. Poger, W.F. Van Gunsteren, A.E. Mark, A new force field for simulating phosphatidylcholine bilayers, J. Comput. Chem., 31 (2010) 1117-1125.
[65] H.J.C. Berendsen, J.P.M. Postma, W.F. van Gunsteren, J. Hermans, Interaction models for water in relation to protein hydration, in: B. Pullman (Ed.) Intermolecular forces, vol. 14, Springer Netherlands, 1981, pp. 331-342.
[66] I.G. Tironi, R. Sperb, P.E. Smith, W.F. van Gunsteren, A generalized reaction field method for molecular dynamics simulations, J. Chem. Phys., 102 (1995) 5451-5459.
[67] S. Miyamoto, P.A. Kollman, Settle-analytical version of the shake and rattle algorithm for rigid water models, J. Comput. Chem., 13 (1992) 952-962.
[68] H.J.C. Berendsen, J.P.M. Postma, W.F. van Gunsteren, A. Dinola, J.R. Haak, Molecular dynamics with coupling to an external bath, J. Chem. Phys., 81 (1984) 3684-3690.
[69] W. Humphrey, A. Dalke, K. Schulten, VMD - visual molecular dynamics, J. Mol. Graphics Model., 14 (1996) 33-38.
[70] N. Michaud-Agrawal, E.J. Denning, T.B. Woolf, O. Beckstein, MDAnalysis: A toolkit for the analysis of molecular dynamics simulations, J. Comput. Chem., 32 (2011) 2319-2327.
[71] A.D. Buckingham, Molecular quadrupole moments, Quarterly Reviews, Chemical Society, 13 (1959) 183-214.
[72] D.J. Craik, N.L. Daly, C. Waine, The cystine knot motif in toxins and implications for drug design, Toxicon, 39 (2001) 43-60.
[73] J. Kalia, M. Milescu, J. Salvatierra, J. Wagner, J.K. Klint, G.F. King, B.M. Olivera, F. Bosmans, , From foe to friend: Using animal toxins to investigate ion channel function, J. Mol. Biol., 427 (2015) 158–175.

Table 1. Charge, solvent accessible surface area (SASA) and residual dipole moments of the pore blockers (PB) and of six gating modifiers (GM) with and without phospholipid binding activity. MOA = Mechanism of action.

Peptide	MOA	Phospholipid binding	Charge	Total SASA ($Å^2$)	Hydrophobic SASA (% of total SASA)	Residual dipole moment (Debye)
ShK	PB	No	+7	1510	23%	98
KIIIA	PB	No	+2	2777	61 %	37
Hd1a	GM	No	+3	2931	61 %	295
HuwentoxinIV	GM	No	+4	3148	55 %	206
SGTx1	GM	Yes	+2	2842	47 %	181
Hanatoxin	GM	Yes	+2	3330	50 %	117
VsTx1	GM	Yes	+3	2994	57 %	109
ProTx-I	GM	Yes	+2	2842	47 %	91

Figures

A

Peptide	Sequence	Source[a]	Target[b]	Charge[c]	RT (min)[d]	Inhibition[e]
ShK	RSCIDTIPKSRCTAFGCKHSMKYRLSFCRKTCGTC	*Stichodactyla helianthus*	K_V channels	+7	18.9	Pore blocker
KIIIA	CCNCSSKWCRDHSRCC	*Conus kinoshitai*	Na_V channels	+2	15.8	Pore blocker
Hd1a	ACLGFGKSCNPSNDQCCKSSSLACSTKHKWCKYEL	*Haplopelma doriae*	Na_V channels	+3	22.0	Gating modifier
ProTx-1	ECRYWLGGCSAGQTCCKHLVCSRRHGWCVWDGTFS	*Thrixopelma pruriens*	Na_V K_V and Ca_V channels	+2	26.5	Gating modifier

[a]Animal species expressing the toxin; [b]Channels that have so far been indentified as a target; [c]Overall charge of the peptide at pH 7.4. [d]The retention time (RT) was determined by analytical-HPLC with 2%/min gradient of solvent B (90% acetronitile, 0.1% formic acid against solvent A (0.1% formic acid), this value allows comparison of the oeverall hydrophobicity of the peptides; [e]Type of inhibitor; Black lines show the disulfide connectivity

B

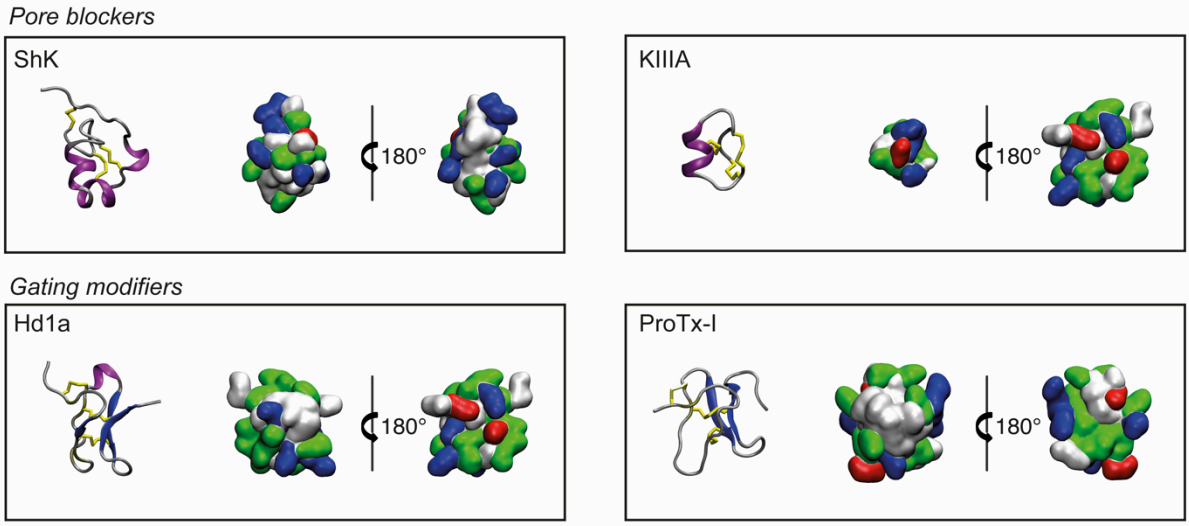

Fig. 1. Sequence and structure of peptides used in this study. (A) Sequence, source, ion channel target, overall charge, RP-HPLC retention time, and type of channel inhibition. Disulfide-bonds are indicated by horizontal lines below the sequences. (B) Three-dimensional structure of the peptides. The ribbon representations on the left are coloured according to secondary structure (α-helices in purple and β-strands in blue), while the surface representations on the right are coloured according to residue type (hydrophobic residues in white, polar (uncharged) residues in green, positively charged residues in blue and negatively charged residues in red).

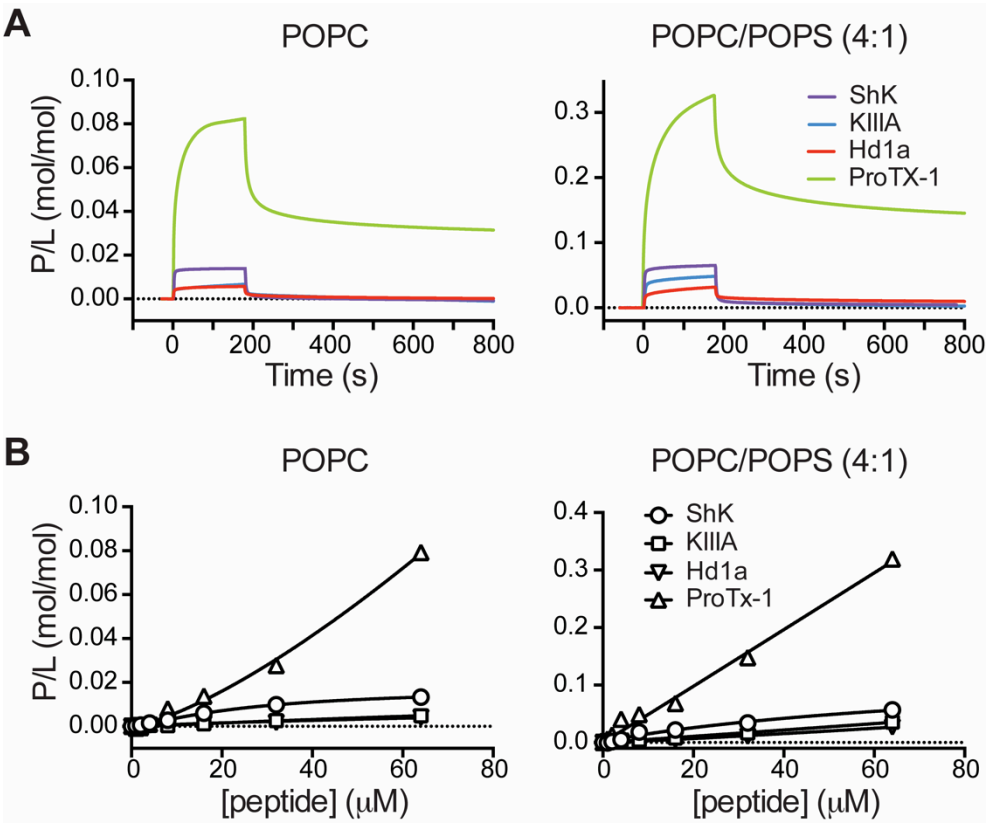

Fig. 2. SPR analysis of lipid binding by pore-blocking and gating-modifier toxins. (A) Sensorgrams obtained upon injection of 64 μM peptide (ShK, KIIIA, ProTx-I or Hd1a) over deposited POPC or POPC/POPS (4:1) bilayers during association (180 s) and dissociation (600 s). Response units (RU) were converted into mass (1 RU ~1 pg/mm^2 of peptide or lipid) and normalised to peptide-to-lipid ratio (mol/mol) in order to allow comparison of the different peptides. This was necessary as the peptides have different molecular weights, and different lipid systems require different amounts of lipid to cover the chip surface. ShK, KIIIA, or Hd1a all display sensorgrams typical of low peptide-lipid binding. ProTx-I shows a high P/L (mol/mol) signal at the end of association and a slow off rate, characteristic of a peptide with affinity for lipid bilayers. (B) Peptide-to-lipid ratio obtained after injection of peptide for 170 s over POPC or POPC/POPS bilayers as a function of the peptide concentration injected.

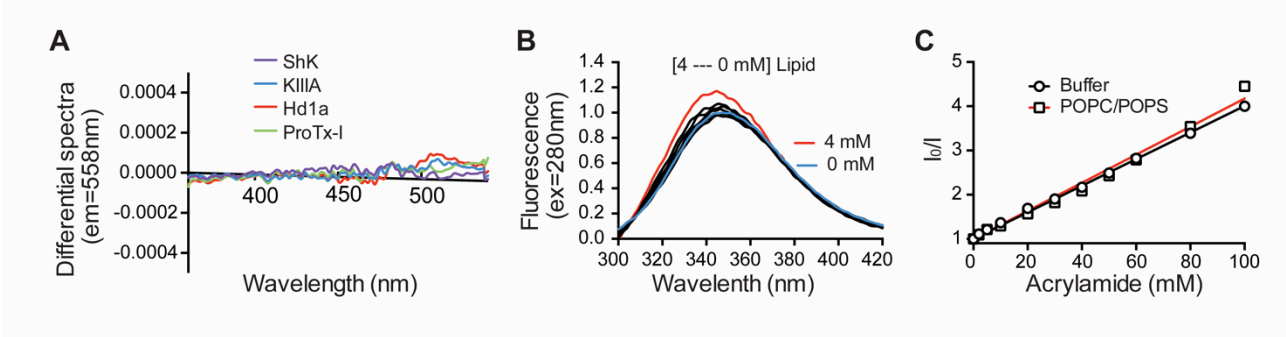

Fig. 3. Examination of peptide insertion into lipid membrane using fluorescence spectroscopy. (A) Di-8-ANEPPS differential excitation spectra obtained with 200 μM of POPC/POPS (4:1) LUVs labelled with 4 μM Di-8-ANEPPS in the presence of 20 μM of ShK, KIIA, H1d1a or ProTx-I. The absence of a shift in the differential spectra suggests no change in the membrane dipolar potential. (B) Fluorescence emission spectra of 25 μM ProTx-I in the absence (blue) and presence of various concentrations of POPC/POPS (4:1) LUVs (0.05, 0.1, 0.2, 0.5, 1, 1.5 and 2 mM are shown in black and 4 mM Lipid is shown in red). No significant blue shift or increase in the quantum yield was found. (C) Acrylamide quenching of fluorescence emission intensity (ex = 290 nm, em =348 nm) of 25 μM ProTx-I in buffer (10 mM HEPES, 150 mM NaCl pH 7.4) or in the presence of 1 mM POPC/POPS (4:1) vesicles. Data are represented as Stern Volmer plots. Calculated K_{SV} is 30.1 ± 0.3 M^{-1} in buffer and 31.7 ± 0.8 M^{-1} in the presence of POPC/POPS (4:1).

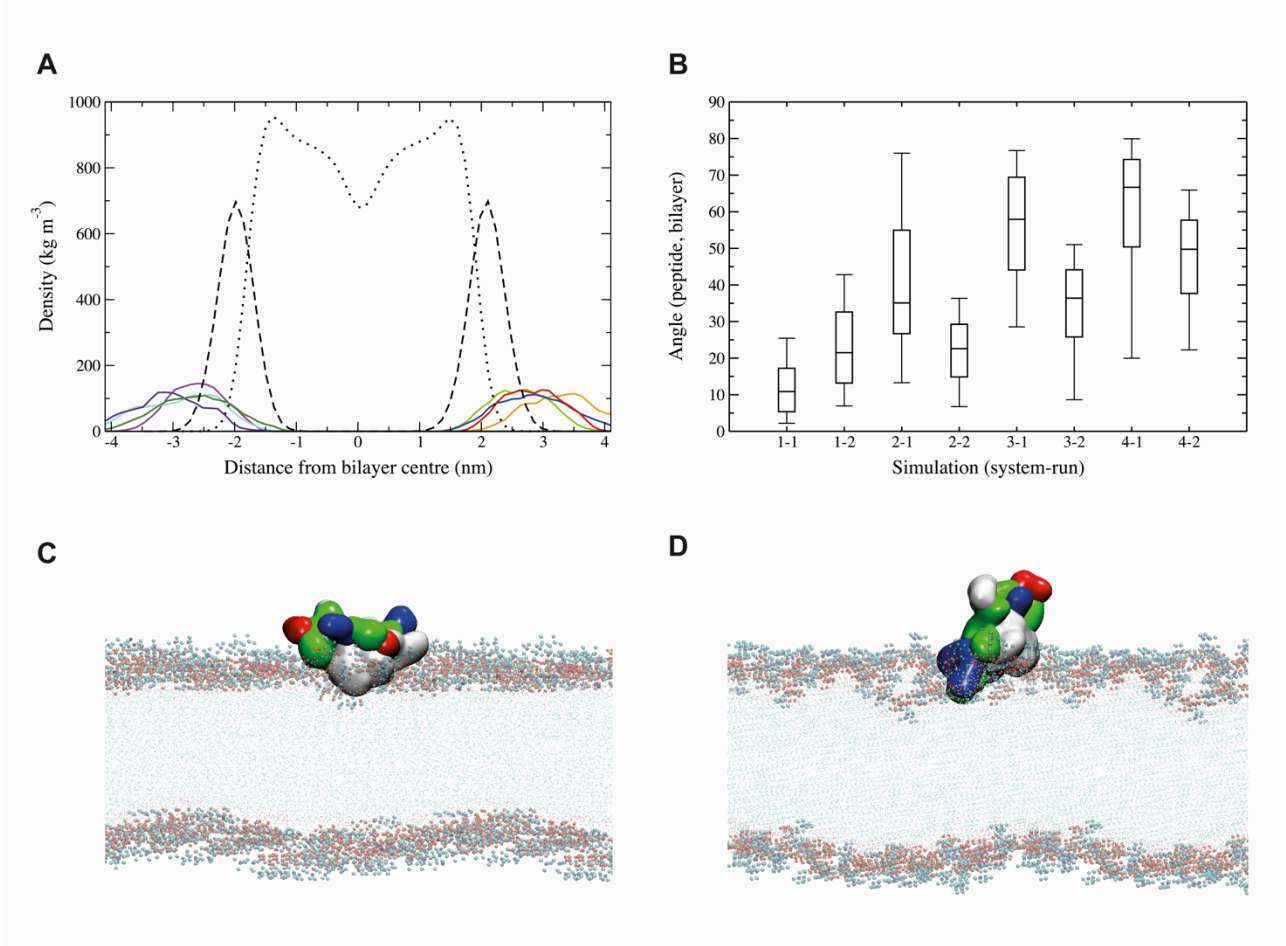

Fig. 4. Position and orientation of ProTx-I in POPC bilayers calculated from MD simulations. (A) Density profile of the POPC lipid bilayer and ProTx-I along the normal of the membrane. Density of lipid head groups (dashed line) and lipid tails (dotted line) were averaged over the eight independent simulations. The density profiles of the peptide were calculated separately for each simulation and are shown in colour. (B) Boxplot showing the angle between the peptide and lipid bilayer surface from eight simulations. Bottom, middle and top of the box represent the 25th, 50th and 75th percentile while whiskers represent the 10th and 90th percentile. (C,D) Snapshots from simulations showing the orientation of the peptide relative to the membrane surface corresponding to angles of ~5° and ~50°. The peptide surface is coloured by residue type (hydrophobic, white; polar, green; positively charged, blue; and negatively charged, red).

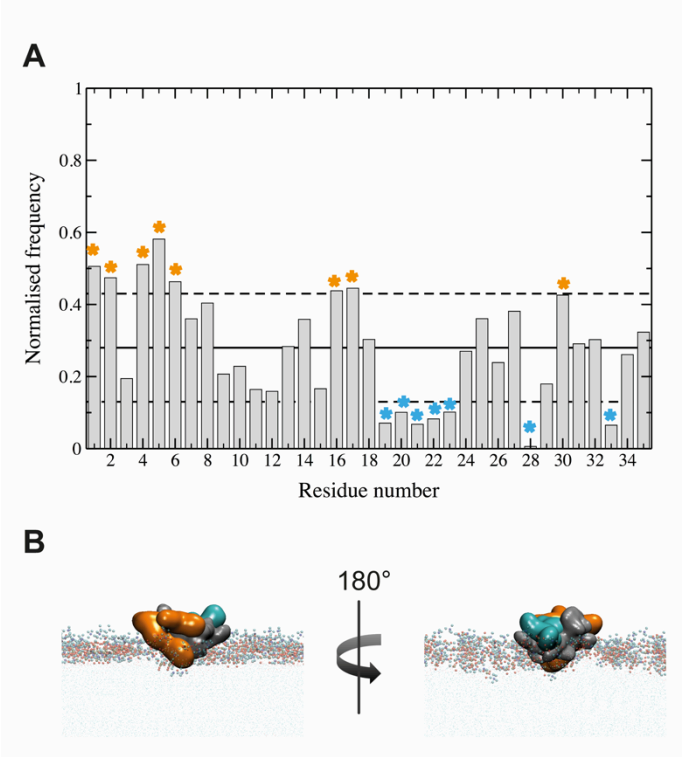

Fig. 5. POPC interaction surface of ProTx-I calculated from MD simulations. (A) Normalised frequency of finding a ProTx-I residue within 0.35 nm of a POPC bilayer calculated from eight independent MD simulations. The lipid-residency frequency averaged over all residues is shown by the solid horizontal line, while the dashed lines indicate ± one standard deviation from the average. Residues with a normalised frequency below or above one standard deviation from the average are marked with a cyan or orange asterisk, respectively. Glu1, Cys2, Tyr4, Trp5, Cys16, Lys17 and Trp30 are more likely to contact the lipid bilayer, while residues Leu19, Val20, Cys21, Ser22, Arg23, Cys28 and Thr33 are more likely to point away from the membrane. (B) Snapshots from MD simulations showing the orientation of ProTx-I relative to the membrane; residues that are more or less likely to contact the lipid bilayer surface are coloured orange and cyan, respectively.

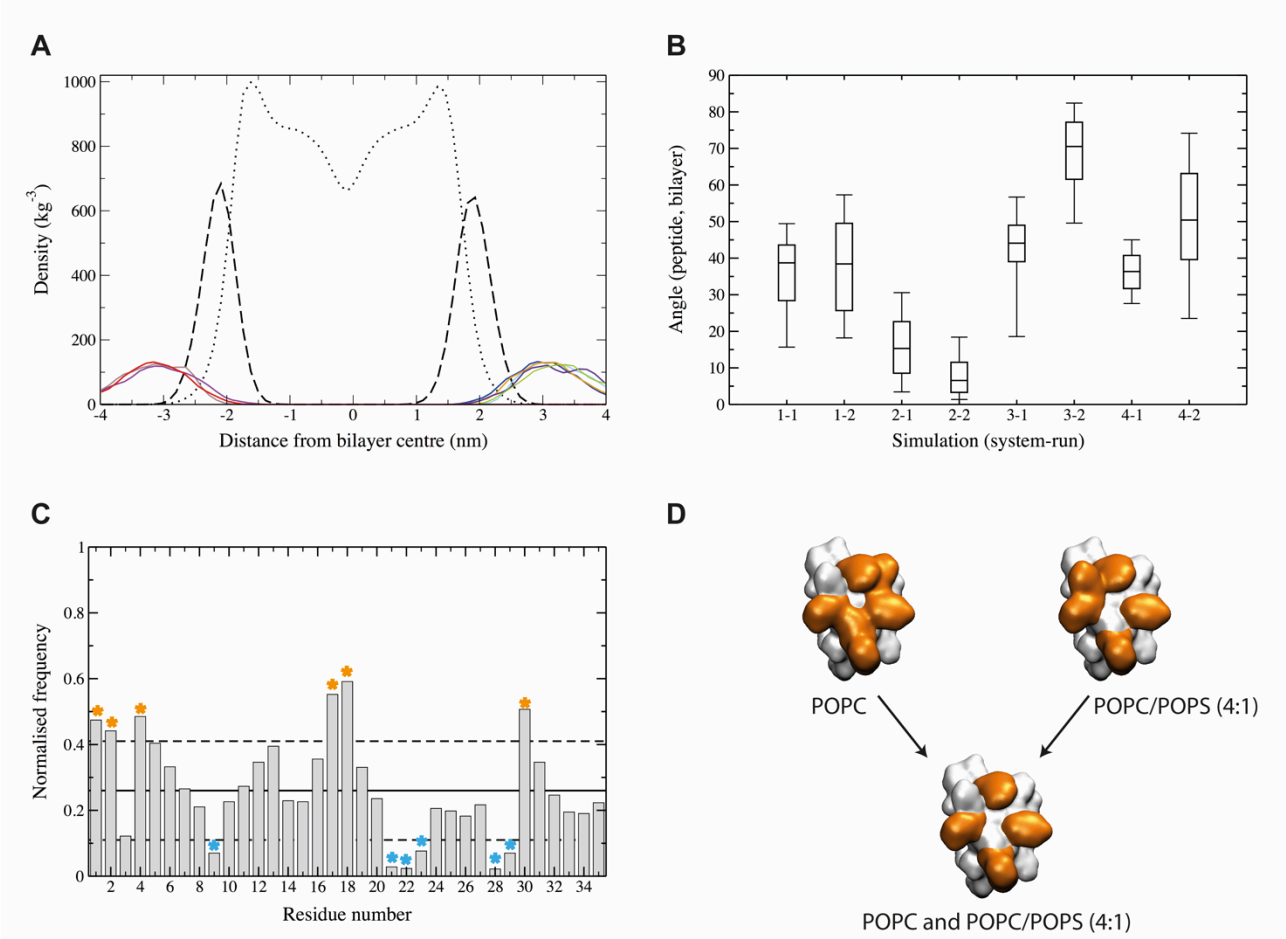

Fig. 6. Position and orientation of ProTx-I in POPC/POPS bilayers calculated from MD simulations. (A) Density profile of the POPC/POPS lipid bilayer and ProTx-I along the normal of the membrane. Density of lipid head groups (dashed line) and lipid tails (dotted line) were averaged over the eight independent simulations. Density profiles of the peptide were calculated separately for each simulation and are shown in colour. (B) Boxplot showing the angle between the peptide and lipid bilayer surface from eight simulations. Bottom, middle and top of the box represent the 25th, 50th and 75th percentile, respectively. Whiskers represent the 10th and 90th percentile. (C) Normalised frequency of finding a residue within 0.35 nm of the lipid bilayer calculated from the combined MD simulations. The lipid-residency frequency averaged over all residues is shown by the solid horizontal line, while the dashed lines indicate ± one standard deviation from the average. Residues with a normalised frequency below or above one standard deviation from the average are marked with a cyan or orange asterisk, respectively. Glu1, Cys2, Tyr4, Lys17, His18 and Trp30 are more likely to contact the lipid bilayer, while residues Cys9, Cys21, Ser22, Arg23, Cys28 and Val29 are less likely to be close to the membrane. (D) Surface

representation of ProTx-I with residues more or less likely to contact the lipid bilayer shown in orange and cyan, respectively. Solid coloured residues are part of the interaction surface in simulations of ProTx-I in the presence of both a pure POPC bilayer and a POPC/POPS (4:1) bilayer.

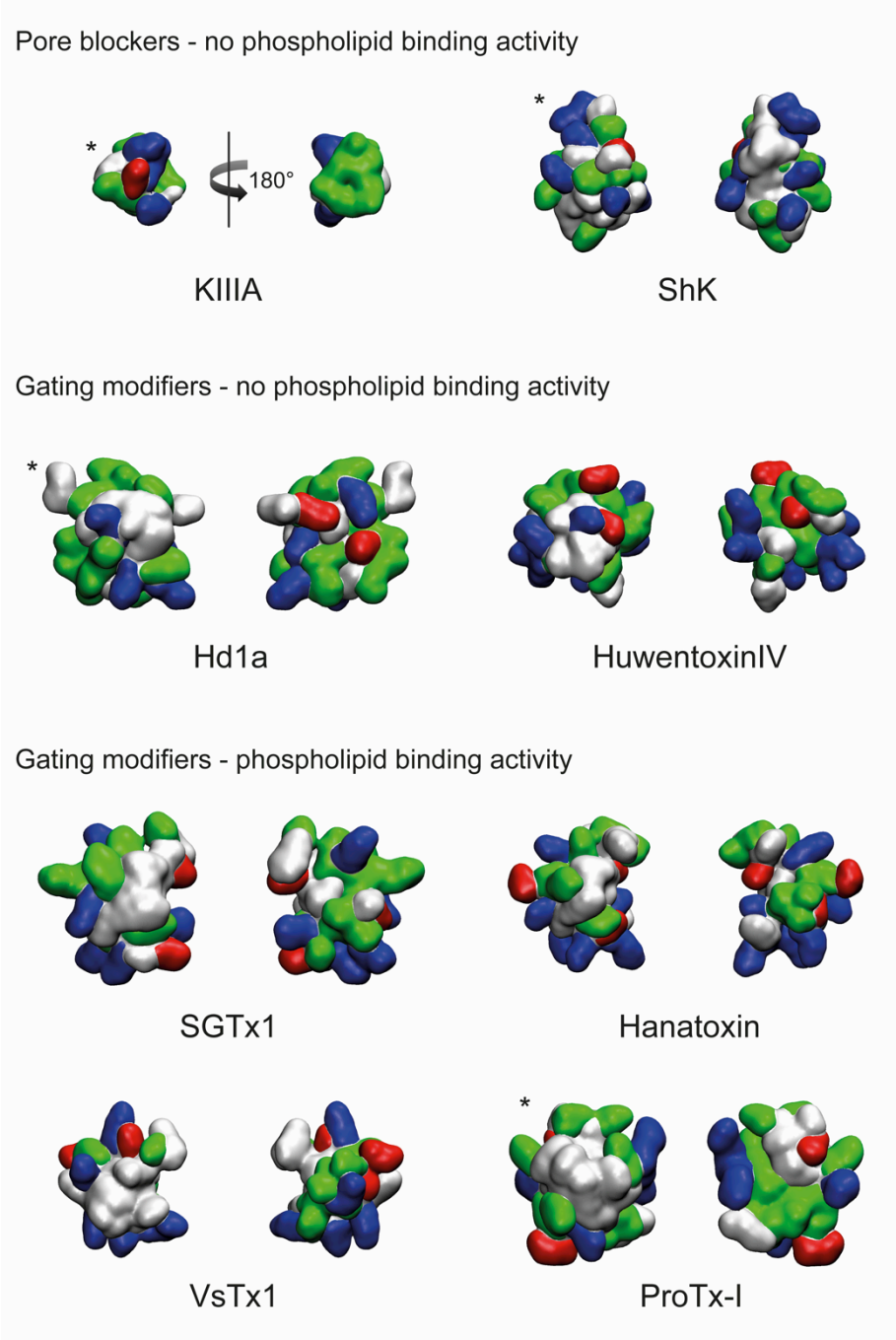

Fig. 7. Comparison of pore blockers and gating modifiers with and without phospholipid binding activity. Peptides are shown in surface representation and coloured by residue type (hydrophobic, white; polar (uncharged), green; positively charged, blue; and negatively charged, red). The phospholipid binding activity of peptides marked with an asterisk are based on results from this study. The phospholipid binding activities of VsTx1 [27], SGTx1 [28, 29], hanatoxin [29, 30] and huwentoxin IV [32] were reported in previous studies.